

Effect of chromosomal integration on catalytic performance of a multi-component P450 system in *Escherichia coli*

U. Joost Luelf¹ | Lisa M. Böhmer¹ | Shengying Li² | Vlada B. Urlacher¹ 

¹Institute of Biochemistry, Heinrich-Heine University Düsseldorf, Düsseldorf, Germany

²State Key Laboratory of Microbial Technology, Shandong University, Qingdao, Shandong, China

Correspondence

Vlada B. Urlacher, Institute of Biochemistry, Heinrich-Heine University Düsseldorf, 40225 Düsseldorf, Germany.
Email: vlada.urlacher@uni-duesseldorf.de

Funding information

European Regional Development Fund (EFRE), Project "ClusterIndustrial Biotechnology (CLIB) Kompetenzzentrum Biotechnologie (CKB)

Abstract

Cytochromes P450 are useful biocatalysts in synthetic chemistry and important bio-bricks in synthetic biology. Almost all bacterial P450s require separate redox partners for their activity, which are often expressed in recombinant *Escherichia coli* using multiple plasmids. However, the application of CRISPR/Cas recombineering facilitated chromosomal integration of heterologous genes which enables more stable and tunable expression of multi-component P450 systems for whole-cell biotransformations. Herein, we compared three *E. coli* strains W3110, JM109, and BL21(DE3) harboring three heterologous genes encoding a P450 and two redox partners either on plasmids or after chromosomal integration in two genomic loci. Both loci proved to be reliable and comparable for the model regio- and stereoselective two-step oxidation of (*S*)-ketamine. Furthermore, the CRISPR/Cas-assisted integration of the T7 RNA polymerase gene enabled an easy extension of T7 expression strains. Higher titers of soluble active P450 were achieved in *E. coli* harboring a single chromosomal copy of the P450 gene compared to *E. coli* carrying a medium copy pET plasmid. In addition, improved expression of both redox partners after chromosomal integration resulted in up to 80% higher (*S*)-ketamine conversion and more than fourfold increase in total turnover numbers.

KEYWORDS

chromosomal integration, CRISPR/Cas9, cytochrome P450, episomal expression, redox partners, whole-cell catalyst

1 | INTRODUCTION

Selective oxidation of complex compounds is an important step towards their functionalization in synthetic chemistry and structural diversification during biosynthesis. Several enzymes enable C–H bond oxidation, including α -ketoglutarate-dependent hydroxylases, dioxygenases and unspecific peroxygenases (Aranda et al., 2021). However, cytochrome P450 monooxygenases (P450s or CYPs)

currently remain unsurpassed regarding their broad substrate and reaction spectra as well as their targeted specificity. In this context, P450-catalyzed reactions often represent key steps in biosynthetic pathways as well as artificial multienzyme cascades (Fessner, 2019). Two well-known examples are the synthesis of a precursor of the chemotherapeutic drug taxol in *Escherichia coli* (Ajikumar et al., 2010) and the production of a precursor of the antimalarial drug artemisinin in *Saccharomyces cerevisiae* (Ro et al., 2006). Due to these properties,

Dedicated to Karl-Erich Jaeger for his outstanding contributions in the field of molecular enzyme technology.

This is an open access article under the terms of the Creative Commons Attribution-NonCommercial-NoDerivs License, which permits use and distribution in any medium, provided the original work is properly cited, the use is non-commercial and no modifications or adaptations are made.

© 2023 The Authors. *Biotechnology and Bioengineering* published by Wiley Periodicals LLC.

P450s have been recognized not only as useful biocatalysts for organic chemistry but also as important bio-bricks in synthetic biology (Urlacher & Girhard, 2019).

P450s are normally dependent on the cofactor NAD(P)H and on redox partner proteins which transfer electrons from NAD(P)H to the heme group and thus almost always function as multi-component systems (Hannemann et al., 2007; Li et al., 2020). After substrate binding, ferric (Fe^{3+}) heme iron is reduced by redox partners via one electron reduction to ferrous (Fe^{2+}) form, which binds molecular oxygen. After the second one-electron reduction by the redox partners and two protonation steps, the dioxygen bond is cleaved, yielding the reactive ferryl-oxo species Compound I and water as byproduct. The Compound I is considered the main active species in P450 reactions (Belcher et al., 2014). Traditionally, microorganisms harboring P450s and their cognate redox partner proteins have been used since the 1960s to produce oxidized compounds like hydrocortisone or pravastatin at industrial scale (Park et al., 2003; Petzoldt et al., 1982). After introducing recombinant DNA technology, heterologous microbial hosts have become more attractive as whole-cell biocatalysts or microbial cell factories with better control over enzyme activities and costs. For P450-catalyzed reactions, *E. coli* seems to be a particularly appropriate host because it is easy to manipulate and does not express intrinsic P450s (Brixius-Anderko et al., 2015). Metabolic pathways and gene expression in *E. coli* are extensively studied, and a number of commercial expression strains as well as a variety of genetic engineering methods are available (Pontrelli et al., 2018).

In *E. coli*, heterologous gene expression is often accomplished using episomal (plasmid-based) systems. Such systems generally have several advantages like easy cloning and gene manipulation including protein engineering. Nevertheless, there are also a few drawbacks, particularly when antibiotic resistance genes are used as selectable markers to maintain plasmids within the host. Apart from the negative impact on further emergence of antibiotic resistance, the use of antibiotics often affects cell growth. Furthermore, multiple high copy plasmids may lead to the expression heterogeneity and contribute to the high transcriptional metabolic burden (Ajikumar et al., 2010; Birnbaum & Bailey, 1991; Mairhofer et al., 2013). In contrast, chromosomal integration of heterologous genes eliminates the need for antibiotics while maintaining stable expression and reducing the transcriptional metabolic burden which can result in similar or even higher enzyme activities and increased metabolite production compared to plasmid-based systems (Englaender et al., 2017; Mairhofer et al., 2013; Wang et al., 2016). The adaption of the CRISPR/Cas system for *E. coli* has expedited genome editing including chromosomal integration (Jiang et al., 2015), and its combination with λ -Red recombineering has been reported several times for *E. coli* (Dong et al., 2021; Ou et al., 2018). In contrast to the λ -Red recombineering method originally described by Datsenko and Wanner (2000), CRISPR/Cas-assisted recombineering can be designed “scarless” which facilitates iterative genome editing, because it excludes the risk of undesired genomic rearrangements (Reisch & Prather, 2015).

While examples of the use of *E. coli* strains with chromosomally integrated genes or even metabolic pathways are still less common than plasmid-based systems, to our knowledge, no direct comparison between plasmid-based and chromosomal expression for P450-catalyzed biotransformations has been described yet. In this regard, it is not only important to achieve high P450 expression levels, but also to balance its concentration with those of the redox partners because their ratios affect the conversion efficiency (Bakkes et al., 2017; Khatri et al., 2017; Liu et al., 2022). To perform such a comparison, we chose a variant of CYP154E1 from *Thermobifida fusca* YX (further referred to as CYP154E1 QAA) supported by two redox partners—the flavodoxin YkuN from *Bacillus subtilis* and the FAD-containing reductase FdR from *E. coli*—as a three-component model P450 system. In our previous study, the YkuN/FdR couple was selected as the most appropriate for reconstituting CYP154E1 activity among several heterologous redox partners (von Bühler et al., 2013). CYP154E1 was recently engineered by mutagenesis to catalyze a two-step conversion of (*S*)-ketamine via the highly chemoselective *N*-demethylation and the regio- and stereoselective C6-hydroxylation to (2*S*,6*S*)-hydroxynorketamine, which is considered a potential antidepressant (Bokel et al., 2020; Zanos et al., 2016, 2018) (Scheme 1).

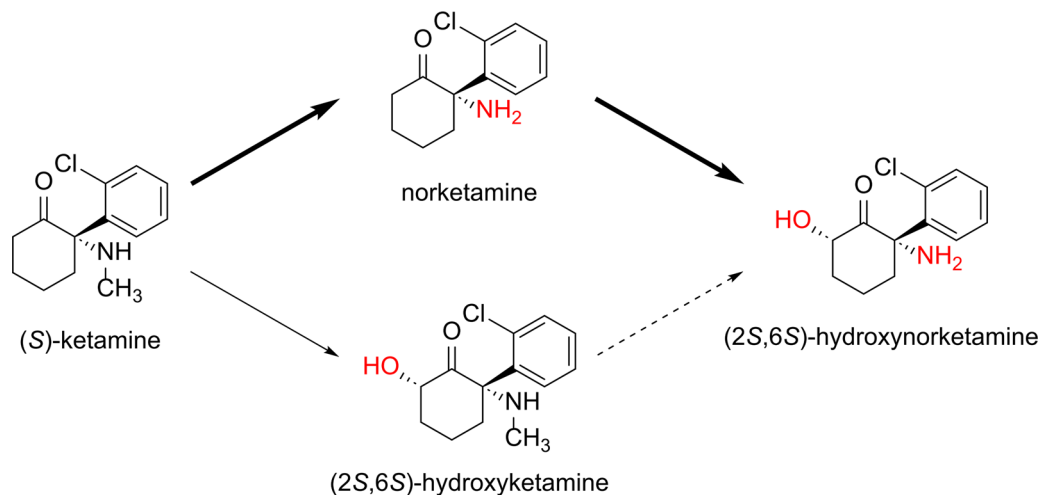
In our previous work, a two-plasmid system harboring all three genes under control of the T7 promoter was established, and whole cells were used for this biotransformation (Bokel et al., 2020). However, T7 expression requires the presence of the phage T7 RNA polymerase (T7RNAP) which thus limits the choice of expression strains. Therefore, the commercial, engineered *E. coli* B strain BL21(DE3) as well as its derivatives, among others, are commonly used (Dumon-Seignovert et al., 2004; Miroux & Walker, 1996). In contrast, the number of commercially available K-12 strains which are suitable for T7 expression is, however, very limited. Hence, the first step of this study was the CRISPR/Cas-assisted chromosomal integration of *T7 gene 1* which encodes the T7RNAP into different K-12 strains.

Further, several plasmid-free recombinant strains were constructed, in which the three genes encoding CYP154E1 QAA, YkuN and FdR were integrated combinatorially into different genomic loci. Particular focus was placed on the experimental design for fast PCR-based synthesis of the linear donor DNA template for homologous recombination. This method facilitates the step from plasmid-based to plasmid-free biotransformations using existing pET vector-based libraries as a starting point. Finally, episomal and chromosomal expression for efficient two-step whole-cell biotransformation of (*S*)-ketamine to (2*S*,6*S*)-hydroxynorketamine were compared.

2 | MATERIALS AND METHODS

2.1 | Strains and plasmids

E. coli DH5 α (Clontech) was used for cloning and plasmid propagation. *E. coli* BL21(DE3) (Novagen), *E. coli* JM109 (NEB) and *E. coli*



SCHEME 1 Consecutive two-step oxidation of (S)-ketamine to (2S,6S)-hydroxynorketamine catalyzed by the CYP154E1 QAA variant. Time-course studies have revealed a high preference (indicated by bold arrows) of oxidative *N*-demethylation followed by hydroxylation rather than the other way around (Bokel et al., 2020).

W3110 (DSMZ) were used for genome engineering, expression and whole-cell conversion. pET-16b YkuN, pET-28a(+) CYP154E1 QAA (includes N-terminal 6xHis tag), pET-22b(+) CYP154E1 QAA (without His tag) and pCOLADuet YkuN (I) FdR (II) were described in previous studies (Bokel et al., 2020; Girhard et al., 2010) and served as templates to construct donor DNA for chromosomal integration or were used for episomal expression, respectively. Plasmids pCas (Addgene plasmid #62225) (Jiang et al., 2015), pEcCas (Addgene plasmid #73227) (Li et al., 2021), and pgRNA-bacteria (hereinafter referred to as “pgRNA,” Addgene plasmid #44251) (Qi et al., 2013) were derived from Addgene. A complete list of all primers, strains, and plasmids used in this study can be found in the Supporting Information (Tables S1–S3).

2.2 | Verification of Lon protease deficiency in *E. coli* JM109

Primers binding upstream and downstream of the region which expected to harbor the *lopA* gene (encoding Lon protease) in *E. coli* JM109 (cf. Table S1) were designed based on the genome sequence of *E. coli* W3110 (GenBank accession no. AP009048.1). The PCR product was then sequenced using Sanger sequencing (Eurofins Genomics).

2.3 | Chromosomal integration

CRISPR/Cas-assisted chromosomal integration was carried out by adapting the protocol originally described by Jiang et al. (2015). Evaluation and design of guide RNAs (gRNAs) for CRISPR/Cas-assisted genome engineering were performed using the CHOPCHOP v3 web tool (Labun et al., 2019) except for the gRNA targeting the

locus *nupG* in K-12 strains which was previously described by Bassalo et al. (2016). Due to a single mutation, a slightly different targeting sequence had to be used in B strains as compared to K-12 strains for this locus (cf. Table S1). To substitute the N_{20} targeting sequence of the aforementioned plasmid pgRNA, a PCR followed by restriction digestion with FastDigest™ BcuI (SpeI) and DpnI (Thermo Scientific) and a self-circularization ligation step was carried out as described by Seo et al. (2017). Successful gRNA substitution was verified by Sanger sequencing (Eurofins Genomics).

Homology arms (~500 bp) for λ -Red-mediated homologous recombination were designed using the genome sequences of *E. coli* W3110 (GenBank accession no. AP009048.1) and *E. coli* BL21(DE3) (GenBank accession no. CP001509.3) and were amplified by PCR from boiled cells. *T7 gene 1* (encodes T7 RNA polymerase for integration in K-12 strains) was amplified from boiled cells of *E. coli* BL21(DE3) as well. Other genes for integration were amplified from pET-28a(+) CYP154E1 QAA, pET-16b YkuN, and pCOLADuet YkuN (I) FdR (II), respectively. Double-stranded donor DNA (dsDonorDNA) for homologous recombination was generated by fusion PCR of homology arms and the gene(s) of interest (cf. Figure S1). Fusion PCR contained 50 ng of the amplified gene and equimolar amounts of the homology arms as well as 0.5 μ M of the outermost primers (cf. Table S1) in 50 μ L total reaction volume. The further composition of the samples was prepared according to the manufacturer's protocol for Phusion™ DNA polymerase (Thermo Scientific).

For preparation of electrocompetent cells, 5 mL 2xYT medium (30 μ g/mL kanamycin) were inoculated with 100 μ L of an overnight culture harboring either pCas (in case of W3110) or the updated plasmid version pEcCas (in BL21(DE3) and JM109), which was designed to improve genome editing in BL21(DE3) (Li et al., 2021). For induction of λ -Red genes, 100 μ L 1 M L-arabinose were added and the cultures were incubated at 30°C (pCas) or 37°C (pEcCas), 200 revolutions per minute (rpm) for 2 h (pEcCas) or 4 h (pCas),

respectively. After cell harvesting by centrifugation, the cells were washed twice with 1 mL ice-cold 10% (vol/vol) glycerol (cell pellet resuspended, 10 min incubation on ice, centrifugation). Finally, the cell pellet was resuspended in 100 μ L ice-cold 10% (vol/vol) glycerol. After addition of 100 ng pgRNA and approximately 500 ng donor dsDonorDNA, electroporation was performed in a 2 mm gap electroporation cuvette at 2.5 kV (MicroPulser™ electroporator from Bio-Rad). The cells were suspended immediately in 1 mL of ice-cold 2xYT or SOC medium and recovered for 1–2 h at 30°C (pCas) or 37°C (pEcCas), respectively. Subsequently, the cells were plated out on LB agar plates (100 μ g/mL ampicillin, 30 μ g/mL kanamycin) and incubated overnight. Successful genome engineering was verified by colony PCR. Curing of pgRNA plasmid, while maintaining pCas/pEcCas for iterative genome engineering, was performed in 5 mL LB medium either by addition of 0.5 mM IPTG (pCas) or 10 mM L-rhamnose (pEcCas). For curing of pCas/pEcCas plasmids, incubation at 42°C, 180 rpm (pCas) or addition of 5% (wt/vol) sucrose (pEcCas) and subsequent incubation at 37°C, 180 rpm were performed (in some cases this step needed to be repeated at 42°C). After streaking, single colonies were tested for antibiotic resistance to obtain cured strains.

2.4 | Expression and biotransformation

For evaluation purposes, P450 expression was carried out in 50 mL Terrific Broth (TB) medium in 500 mL Erlenmeyer flasks. Episomal expression required 30 μ g/mL kanamycin for maintaining the pET-28a(+) plasmid. After inoculation with 1 mL of an overnight culture, the expression cultures were incubated at 37°C, 180 rpm until an optical density (OD₆₀₀) of 0.6–0.8 was reached. Transcription was induced by adding 0.1 mM IPTG. To support heme production, 0.1 mM FeSO₄ as well as 0.5 mM 5-aminolevulinic acid were supplemented. After incubation at 25°C, 140 rpm for 24 h, the cells were harvested by centrifugation. The pellet was resuspended in 4 mL 100 mM potassium phosphate buffer (pH 7.5) per gram cell wet weight for cell disruption by sonication. Cell debris was separated by centrifugation and the soluble fraction was used for P450 quantification by carbon monoxide (CO) difference spectra as described by Omura & Sato, (1964a, 1964b). In addition, sodium dodecyl sulfate–polyacrylamide gel electrophoresis (SDS-PAGE) analysis of both the soluble and insoluble fractions after cell disruption was performed.

Coexpression of P450 and redox partners was carried out in autoinduction medium (100 mL TB medium containing 0.1 mM FeSO₄ and 0.5 mM 5-aminolevulinic acid, 2 mL “50 × 5052,” 2 mL “50 × M” as described by Studier, 2014). Episomal expression required 100 μ g/mL ampicillin and 30 μ g/mL kanamycin for maintaining the plasmids pET-22b(+) and pCOLADuet. After inoculation with 2 mL of an overnight culture, expression cultures were incubated at 37°C, 180 rpm until an OD₆₀₀ of approximately 1.0 was reached. After incubation at 25°C, 120 rpm for 20 h, the cultures were split in half and harvested by centrifugation. One half was

treated as described above. The other half was washed once with PSE buffer (6.75 g/L KH₂PO₄, 85.5 g/L sucrose, 0.93 g/L EDTA-Na₂·2 H₂O, pH 7.5), adjusted to a cell density of 50 mg/mL and stored at –80°C for at least 24 h.

Whole-cell conversion was carried out in 500 μ L scale for which 465 μ L of cell suspension were thawed. After addition of 25 μ L nutrient solution (0.12 M glucose, 0.12 M lactose, 0.24 M sodium citrate in PSE buffer) and 10 μ L 100 mM (S)-ketamine (2 mM final concentration), the reaction mixture was incubated at 25°C, 1200 rpm for 20 h. Extraction was performed with ethyl acetate after adding sodium carbonate and the internal standard xylazine as described by Bokel et al. (2020). The organic solvent was evaporated, and the residue was resuspended in a mixture of acetonitrile and water. Product formation was quantified by LC/MS analysis (LCMS-2020, Shimadzu; Chromolith Performance RP-8e 100–4.6 mm column and Chromolith RP-8e 5–4.6 mm guard cartridge, Merck Millipore) as described before (Bokel et al., 2020).

3 | RESULTS AND DISCUSSION

3.1 | Enabling T7 expression in K-12 strains

The number of commercially available K-12 strains which are suitable for T7-based expression is very limited, although *E. coli* K-12 strains appear to be more easily manipulated by genome editing methods and show occasionally beneficial characteristics in comparison to B strains like lower sensitivity to stress and tolerance to lower oxygen levels (Kang et al., 2002; Yoon et al., 2012). Thus, we chose the *E. coli* K-12 strains W3110 and JM109 for the integration of T7 gene 1. W3110 is an industrially used strain which is closely related to the ancestral K-12 strain (Hayashi et al., 2006; Kang et al., 2002). By selecting JM109, we aimed to combine the high editing efficiency of K-12 strains with improved heterologous protein production due to the lack of Lon protease. The Lon protease encoded by *lopA* gene contributes to degradation of foreign proteins, making Lon-protease-deficient strains such as BL21(DE3) commonly preferred for heterologous gene expression (SaiSree et al., 2001). Lon protease deficiency in JM109 due to IS186 transposon insertion was first mentioned at the OpenWetWare website (Richter et al., 2019) and confirmed in this study by sequencing the region of the *lopA* gene promoter (Figure S2). Very recently, the complete genome sequence of the JM109 strain was uploaded to GenBank (accession no. CP117962.1) and revealed this transposon insertion and the absence of a second copy of *lopA*.

The BL21(DE3) strain for T7 expression was originally constructed by cloning T7 gene 1 into a lambda phage derivative and subsequent lysogenization of BL21 (Studier & Moffatt, 1986). Nowadays, advances in genome editing allow targeted integration without lysogenization which avoids the consequent integration of irrelevant phage genes. Since expression levels of chromosomally integrated genes depend on their integration site (Bryant et al., 2014; Englaender et al., 2017), T7 gene 1 was integrated between the genes

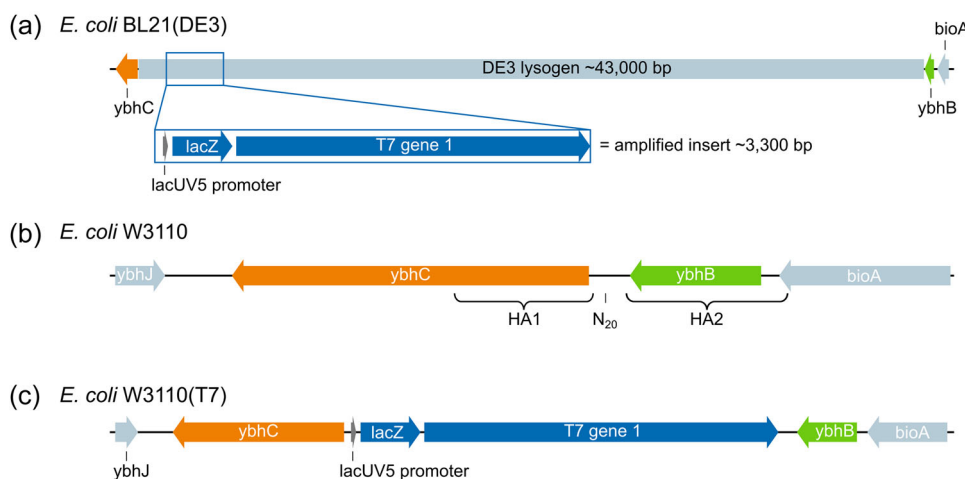


FIGURE 1 Construction of the *Escherichia coli* W3110(T7) strain. (a) *T7 gene 1* (encoding T7 RNA polymerase) under control of lacUV5 promoter and a lacZ fragment located between promoter and *T7 gene 1* were amplified from the DE3 lysogen of *E. coli* BL21(DE3). (b) Gene map of the insertion site in *E. coli* W3110 and design of the 500 bp homology arms (HA1 and HA2) for homologous recombination upstream and downstream of the N₂₀ target sequence for CRISPR/Cas cleavage. (c) Gene map of *E. coli* W3110(T7) showing the integration of *T7 gene 1* between the genes *ybhC* (orange) and *ybhB* (green) comparable to *E. coli* BL21(DE3).

ybhB and *ybhC* as seen in commercial BL21(DE3) to ensure comparability (Figure 1). To this end, *T7 gene 1* under control of the lacUV5 promoter was amplified from the genome of *E. coli* BL21(DE3) and integrated into both K-12 strains using CRISPR/Cas9-assisted recombineering. Integration of a second copy of the *lacI* gene, which is also located in the DE3 lysogen of BL21(DE3), was omitted because we suggested that the copy present in the lac operon is sufficient to repress transcription of single chromosomal copies of heterologous genes. This approach was also described by another group and did not result in higher basal plasmid-based expression (Ting et al., 2020). The constructed K-12 strains harboring a chromosomal copy of *T7 gene 1* are hereafter referred to as W3110(T7) and JM109(T7).

3.2 | Effect of Lon protease deficiency on CRISPR/Cas-assisted genome engineering

Besides our efforts to enable T7 expression in K-12 strains, the use of an updated version of the plasmid pCas—so-called pEcCas—improved genome editing in BL21(DE3) (Li et al., 2021), so that in the following all three *E. coli* strains—W3110(T7) and JM109(T7) as well as BL21(DE3)—were compared. However, it should be noted that the integration efficiency in BL21(DE3) remains low compared to W3110. Surprisingly, the observed integration efficiency in JM109 was equally low (data not shown) as in BL21(DE3), although K-12 strains are reported to show higher integration efficiencies than B strains (Chung et al., 2017; Li et al., 2019). This might be due to a negative effect of the Lon protease deficiency on the efficiency of CRISPR/Cas-assisted chromosomal integration, which was very recently reported by Okshevsky et al. (2023). In addition to its contribution to the degradation of improperly folded proteins, the

Lon protease plays a critical role in the SOS response to DNA damage in cells (Gottesman, 1996). It is likely that the expression of the *lopA* gene explains the differences between BL21(DE3), JM109, and W3110 in our study, rather than the fact that one is a B strain, and the others K-12 strains. When choosing a strain for chromosomal integration and subsequent expression of heterologous genes, it should be considered whether the lack of Lon protease is crucial to produce recombinant proteins or whether high integration efficiency is more important.

3.3 | Integration procedure, integration loci, and donor DNA design

For integration of the *cyp154e1m* gene coding for the target CYP154E1 QAA enzyme, two genomic loci previously described in literature and located similarly close to the origin of replication were evaluated. The gene-disrupting integration of the green fluorescent protein gene (*gfp*) into *nupG* (encoding a nucleoside permease) described by Bassalo et al. (2016) resulted in high fluorescence and high integration efficiency. High expression levels after integration in this region were also observed by Bryant et al. (2014) and Goormans et al. (2020). The second integration site, an intergenic region between the genes *atpI* and *gidB* (also known as *rsmG*) was previously described by Englaender et al. (2017) and Goormans et al. (2020) among others.

For chromosomal integration, the entire cassette consisting of the *cyp154e1m* gene under control of the T7 promoter as well as the T7 terminator was amplified from the pET-based plasmid and fused with homology arms for homologous recombination (Figure S1). The primers listed in the supporting information were specially designed for PCR amplification from any pET vector

which contains a f1 origin of replication (indicated by the (+) following the name, e.g. in pET-28a(+)) (Merck KGaA, 2011). In deviation from this, different primers for amplification of the cassettes of pET-16b and pCOLADuet were designed. Thus, these primer sets can be used for donor DNA synthesis and subsequent chromosomal integration of any desired gene available on most pET or pCOLADuet vectors which facilitates the step from plasmid-based to chromosomal expression in *E. coli*. Hence, after successful optimization of properties such as activity, selectivity, and stability of an enzyme by mutagenesis using well-established plasmid-based engineering techniques, stable chromosomal expression of the optimized mutant can be achieved with little effort using the herein described method and primers. It is worthy of note, however, when choosing new integration loci for simultaneous expression of more genes in reaction cascades, it is important to keep in mind that the T7 terminator (T ϕ) is only approximately 70% effective (Merck KGaA, 2011). Potential read-through and overexpression of homologous genes downstream of the integration loci might be toxic to the cells.

3.4 | Comparison of episomal and chromosomal expression of *cyp154e1m*

Expression studies revealed that chromosomal expression of *cyp154e1m* was improved by an N-terminal polyhistidine (6xHis) tag (data not shown). After integration of the *cyp154e1m* gene including the 6xHis tag into the chosen integration loci (*atpI_gidB* and *nupG*) in all three strains, high discrepancies between episomal and chromosomal expression as well as between the different strains were observed (Figure 2). The highest P450 expression level of 246 nmol per gram cell wet weight (cww) or 6600 nmol per liter culture was achieved in strain BL21(DE3) for chromosomal expression. Similar P450 amounts (also for other P450s) are usually only

achieved in high cell density cultivations rather than simple flask cultivation (Pflug et al., 2007). More importantly, the chromosomal integration of *cyp154e1m* increased the titer of soluble P450 by 40% (from 176 ± 23 to 246 ± 23 nmol/g cell wet weight) in strain BL21(DE3) as compared to episomal expression based on pET-28a(+). Englaender et al. (2017) even described a fivefold increase in recombinant mCherry production after integration into the *atpI_gidB* locus compared to a modified pET vector. In our case, this increase can be explained by a stronger episomal expression leading to a high portion of inactive P450 in the insoluble fraction, as revealed by SDS-PAGE analysis (Figure 2b). It is commonly known that overexpression under control of the strong T7 promoter using a high-copy vector may lead to misfolding and aggregation of improperly folded proteins to inclusion bodies in *E. coli* (Hoang et al., 1999). In addition, accumulation of P450 apoprotein which does not contain the prosthetic heme group can occur if protein folding outpaces heme loading (Sudhamsu et al., 2010). A reduction of the gene copy number from up to approximately 40 copies per cell as expected for a pET vector (Merck KGaA, 2011) to a single chromosomal copy reduced the amount of potentially improperly folded, insoluble P450 and, in turn, increased the amount of heme-loaded, soluble enzyme in BL21(DE3).

A moderate increase in P450 amount compared to the episomal system was also observed after chromosomal expression in W3110(T7). The P450 amounts in soluble and insoluble fractions were generally lower compared to BL21(DE3) (Figure 2 and Figure S3). In the literature, integration of *T7 gene 1* into W3110 resulted in higher fluorescence of sfGFP compared to BL21(DE3) (Ting et al., 2020). However, the integration site of the *T7 gene 1* used in our study is different, which does not allow direct comparison. Why P450 expression worked better in BL21(DE3) was not elucidated further in the frame of this study, however, the expression level generally depends on the gene chosen and might vary for different proteins. Furthermore, possible differences in heme

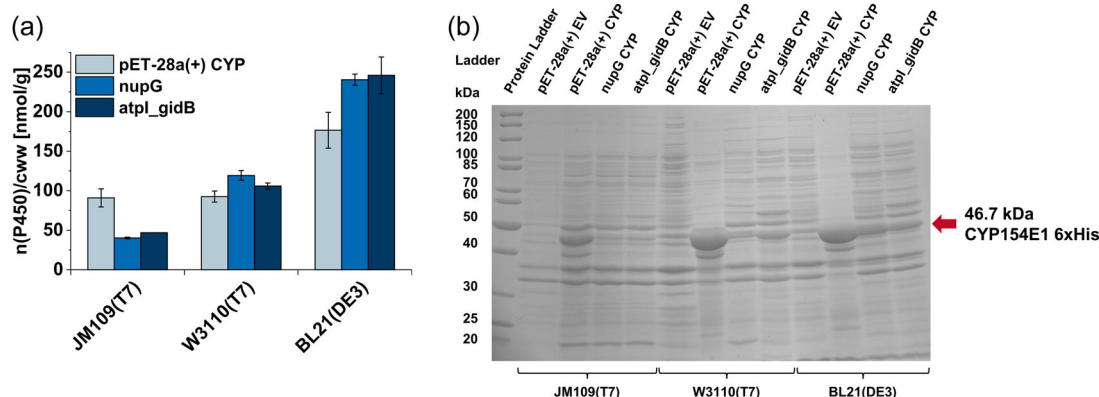


FIGURE 2 Comparison of episomal and chromosomal expression of *cyp154e1m* gene in three *E. coli* strains after induction with 0.1 mM IPTG. Episomal expression was carried out using a pET-28a(+) vector, and chromosomal expression was performed after integration into the loci *nupG* and *atpI_gidB*. (a) Amount of soluble P450 per gram cell wet weight and (b) SDS-PAGE analysis of the insoluble protein fractions after expression and cell disruption. Empty vector (EV) was used as negative control. The expected molecular weight of CYP154E1 QAA (6xHis) is 46.7 kDa.

synthesis or loading in different strains, to the best of our knowledge, have not been investigated so far.

The lowest amount of soluble P450 was measured after chromosomal expression in JM109(T7) (Figure 2a and Figure S3), while after episomal expression, P450 concentration was as high in JM109(T7) as in W3110(T7). Moreover, only in this strain episomal expression resulted in higher concentration of soluble heme-loaded P450 than chromosomal expression. Unexpectedly, less insoluble protein was produced in Lon-deficient JM109(T7) than in W3110(T7), although as mentioned before, Lon protease degrades misfolded proteins. Obviously, Lon protease deficiency is only one feature that can influence heterologous expression in these strains and other factors should be investigated to explain all observed differences between the expression strains used.

Both genomic loci resulted in similar expression levels within the respective strains. In comparison, a previous study by Goormans et al. (2020) reported a slightly higher expression level of GFP in case of the *atpI_gidB* locus compared to the *nupG* locus.

3.5 | Coexpression of redox partners and biotransformation of (S)-ketamine

The strains BL21(DE3) and W3110(T7) were chosen for further experiments. The previously described plasmid-based system consisted of a pET-22b(+) plasmid for *cyp154e1m* expression and a pCOLADuet plasmid for coexpression of *ykuN* and *fdr* (Bokel et al., 2020). This system was not altered and served as the reference system for episomal expression. As described for the integration of the *cyp154e1m* gene, the whole bicistronic operon was amplified from the pCOLADuet vector carrying the *ykuN* and *fdr* genes, and integrated into the locus that was not already occupied by the previously integrated *cyp154e1m* gene (Table 1).

Since the FAD-containing reductase FdR is originating from *E. coli* and in vitro setups for P450-catalyzed reactions usually contain an excess of the flavodoxin/ferredoxin but not the reductase, strains harboring only the *cyp154e1m* and *ykuN* genes without additional integration of the *fdr* gene were also created to investigate whether the endogenous expression of *fdr* is sufficient for the whole-cell biotransformation. After expression, SDS-PAGE analysis of the proteins, biotransformation of 2 mM (S)-ketamine, and quantification of the P450 concentration were performed.

TABLE 1 Bacterial strains with combinatorial integration of *cyp154e1m*, *ykuN*, or *ykuN/fdr*.

Native strain	Combinatorially integrated genes		Label
	<i>atpI_gidB</i> Locus	<i>nupG</i> Locus	
BL21(DE3) or W3110(T7)	<i>cyp154e1m</i>	<i>ykuN</i>	P450-Y
	<i>cyp154e1m</i>	<i>ykuN/fdr</i>	P450-Y/R
	<i>ykuN</i>	<i>cyp154e1m</i>	Y-P450
	<i>ykuN/fdr</i>	<i>cyp154e1m</i>	Y/R-P450

Similar to the case when *cyp154e1m* was expressed alone (Figure 2), an increased P450 expression was observed in BL21(DE3) compared to W3110(T7) (Figure 3). Not only the amount of protein visible on the gel but also the P450 concentrations measured after cell disruption were higher. Higher conversion of (S)-ketamine by the BL21(DE3) strains was observed in comparison to W3110(T7). In this context, lower conversion correlates with high levels of the intermediate norketamine (Scheme 1).

The norketamine intermediate is the main product formed from ketamine by W3110(T7), while in case of BL21(DE3) more of the desired (2S,6S)-HNK was formed (Figure 3c). Remarkably, the turnover numbers of 880–1100 oxidation reactions per P450 calculated for both strains seem comparable, so that differences in product formation and distribution between the strains may be due to different P450 concentrations (Figure 3d).

Consistent with the results shown in Figure 2, which implied high similarity of the two integration loci, it made almost no difference whether the *cyp154e1m* gene was integrated into the *nupG* locus and the redox partners into the *atpI_gidB* locus, or vice versa. Interestingly, in contrast to our previous results, the chromosomal (co)expression of P450 and redox partners resulted in lower P450 concentrations compared to the episomal expression systems in both strains (from 37% up to 64% reduction dependent on the chromosomal system). However, in all cases, simultaneous chromosomal coexpression of *ykuN* and *fdr* resulted in slightly higher P450 amounts compared to the strains where no additional copy of *fdr* was integrated, although the bicistronic operon was expected to increase the transcriptional burden. In addition, a high portion of P450 was found in the insoluble fraction after cell disruption for BL21(DE3), but not in W3110(T7). However, both redox partner proteins were rather soluble in both strains (Figure S4). Even though the highest P450 concentration was achieved after episomal expression (123 ± 7 nmol/g cell wet weight), the highest (S)-ketamine conversion was observed for both strains with all three chromosomally integrated genes (up to 90% (S)-ketamine conversion for BL21(DE3) and up to 46% conversion for W3110(T7)). For strains without additionally integrated copy of *fdr*, lower turnover was observed which implies that the endogenous *fdr* is not sufficient for this biotransformation (Figure 3).

SDS-PAGE analysis revealed higher amounts of the redox partner proteins after chromosomal expression compared to the episomal coexpression, which might explain the lower conversions in the latter despite higher P450 concentrations (Figure 3 and Figure S4). It is commonly observed for P450-catalyzed reactions that the ratio of P450:flavodoxin:reductase has a great influence on the catalytic performance (Bakkes et al., 2017; Khatri et al., 2017). While in in vitro reactions with purified enzymes this ratio can easily be adjusted and fine-tuned, there are only limited possibilities to do so in recombinant microbial hosts. For future optimization, the ratio could either be adjusted by altering the transcription strength using different promoters or by altering the individual copy numbers of the genes. In addition, in case of chromosomal expression, the use of different loci might result in a different expression pattern and subsequent altered catalytic performance.

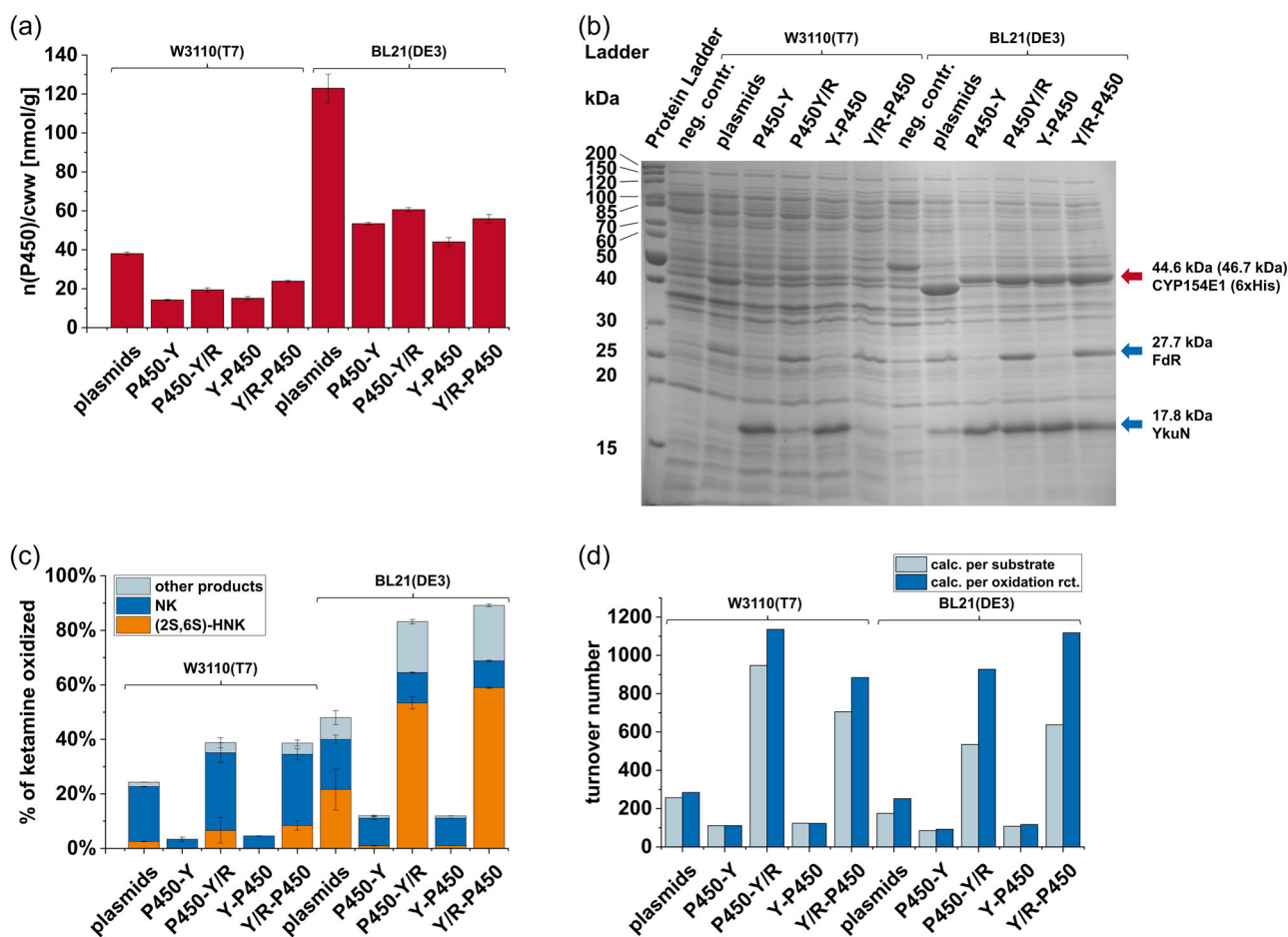


FIGURE 3 Coexpression of P450 and redox partner genes after combinatorial chromosomal integration into two genomic loci (labeling according to Table 1) in comparison to the episomal two-plasmid expression system and whole-cell conversion of 2 mM (*S*)-ketamine. (a) Amount of soluble P450 per gram cell wet weight and (b) SDS-PAGE analysis of whole cells after expression in autoinduction medium. Strains without plasmids or integrated genes were used as negative control. (c) Comparison of product formation ((2*S*,6*S*)-hydroxynorketamine [(2*S*,6*S*)-HNK]), norketamine (NK), and other oxidation products (several hydroxyketamines [HK] and -norketamines [HNK]). (d) Turnover number (TON) was calculated as the number of substrate molecules converted per enzyme (light blue). Since the number of oxidation reactions varies for different products (HK and NK = one oxidation; HNK and dehydronorketamine = two oxidations), an adjusted TON representing the number of oxidation steps catalyzed per enzyme was calculated to account for different product distributions (dark blue).

4 | CONCLUSIONS

In summary, we demonstrated that P450-catalyzed bio-transformation can be performed using *E. coli* cells with chromosomally integrated recombinant genes. When expressed alone, the chromosomally integrated *cyp154e1m* resulted in higher P450 concentration compared to the plasmid-based expression. More importantly, a better-balanced electron transport chain improved (*S*)-ketamine conversion to the potential antidepressant (2*S*,6*S*)-hydroxynorketamine. The two integration loci *nupG* and *atpI_gidB* proved to be reliable and comparable. In addition, the chromosomal integration of T7 RNA polymerase gene enables an easy extension of possible T7 expression strains so that specific advantages of different strains can be combined with strong T7-based expression. In our particular case, the BL21(DE3) strain widely used for protein expression still performed best. This is probably different for other

genes, as it has been described in literature (Ting et al., 2020). The influence of the Lon protease deficiency not only on the production of recombinant proteins, but also on the efficiency of genome engineering should be considered when performing comparable experiments. The primers designed in this study allow easy chromosomal integration of any genes from pET vectors. Chromosomal integration can be regarded as the final step after successful optimization of biocatalysts by mutagenesis to a stable and antibiotic-free expression and biotransformation.

AUTHOR CONTRIBUTIONS

Vlada B. Urlacher and U. Joost Luefl: conceptualized the study. **U. Joost Luefl:** designed and conducted most of the experiments, analyzed the data and prepared the first draft. **Lisa M. Böhmer:** contributed to data acquisition and analysis. **Vlada B. Urlacher and Shengying Li:** contributed to conceiving experiments, interpretation

of data, and writing of the manuscript. All authors edited the manuscript and approved the final version of the manuscript.

ACKNOWLEDGMENTS

We thank Dr. Marco Girhard and Dr. Katja Koschorreck for fruitful discussions. Financial support was provided by the state of North Rhine-Westphalia (NRW) and the "European Regional Development Fund (EFRE)", Project "ClusterIndustrial Biotechnology (CLIB) Kompetenzzentrum Biotechnologie (CKB)" (34.EFRE-0300095/1703FI04). Open Access funding enabled and organized by Projekt DEAL.

CONFLICTS OF INTEREST STATEMENT

The authors declare no conflicts of interest.

DATA AVAILABILITY STATEMENT

The data that support the findings of this study are available from the corresponding author upon reasonable request. Data are available from the corresponding author on reasonable request.

ORCID

Vlada B. Urlacher  <http://orcid.org/0000-0003-1312-4574>

REFERENCES

- Ajikumar, P. K., Xiao, W. H., Tyo, K. E. J., Wang, Y., Simeon, F., Leonard, E., Mucha, O., Phon, T. H., Pfeifer, B., & Stephanopoulos, G. (2010). Isoprenoid pathway optimization for Taxol precursor overproduction in *Escherichia coli*. *Science*, 330(6000), 70–74. <https://doi.org/10.1126/science.1191652>
- Aranda, C., Carro, J., González-Benjumea, A., Babot, E. D., Olmedo, A., Linde, D., Martínez, A. T., & Gutiérrez, A. (2021). Advances in enzymatic oxyfunctionalization of aliphatic compounds. *Biotechnology Advances*, 51, 107703. <https://doi.org/10.1016/j.biotechadv.2021.107703>
- Bakkes, P. J., Riehm, J. L., Sagadin, T., Rühlmann, A., Schubert, P., Biemann, S., Girhard, M., Hutter, M. C., Bernhardt, R., & Urlacher, V. B. (2017). Engineering of versatile redox partner fusions that support monooxygenase activity of functionally diverse cytochrome P450s. *Scientific Reports*, 7(1), 9570. <https://doi.org/10.1038/s41598-017-10075-w>
- Bassalo, M. C., Garst, A. D., Halweg-Edwards, A. L., Grau, W. C., Domaille, D. W., Mutalik, V. K., Arkin, A. P., & Gill, R. T. (2016). Rapid and efficient one-step metabolic pathway integration in *E. coli*. *ACS Synthetic Biology*, 5(7), 561–568. <https://doi.org/10.1021/acssynbio.5b00187>
- Belcher, J., McLean, K. J., Matthews, S., Woodward, L. S., Fisher, K., Rigby, S. E. J., Nelson, D. R., Potts, D., Baynham, M. T., Parker, D. A., Lays, D., & Munro, A. W. (2014). Structure and biochemical properties of the alkene producing cytochrome P450 OleTJE (CYP152L1) from the *Jeotgalicoccus* sp. 8456 bacterium. *Journal of Biological Chemistry*, 289(10), 6535–6550. <https://doi.org/10.1074/jbc.M113.527325>
- Birnbaum, S., & Bailey, J. E. (1991). Plasmid presence changes the relative levels of many host cell proteins and ribosome components in recombinant *Escherichia coli*. *Biotechnology and Bioengineering*, 37(8), 736–745. <https://doi.org/10.1002/bit.260370808>
- Bokel, A., Rühlmann, A., Hutter, M. C., & Urlacher, V. B. (2020). Enzyme-mediated two-step regio- and stereoselective synthesis of potential rapid-acting antidepressant (2S,6S)-hydroxynorketamine. *ACS Catalysis*, 10(7), 4151–4159. <https://doi.org/10.1021/acscatal.9b05384>
- Brixius-Anderko, S., Schiffer, L., Hannemann, F., Janocha, B., & Bernhardt, R. (2015). A CYP21A2 based whole-cell system in *Escherichia coli* for the biotechnological production of premedrol. *Microbial Cell Factories*, 14, 135. <https://doi.org/10.1186/s12934-015-0333-2>
- Bryant, J. A., Sellars, L. E., Busby, S. J. W., & Lee, D. J. (2014). Chromosome position effects on gene expression in *Escherichia coli* K-12. *Nucleic Acids Research*, 42(18), 11383–11392. <https://doi.org/10.1093/nar/gku828>
- Chung, M. E., Yeh, I. H., Sung, L. Y., Wu, M. Y., Chao, Y. P., Ng, I. S., & Hu, Y. C. (2017). Enhanced integration of large DNA into *E. coli* chromosome by CRISPR/Cas9. *Biotechnology and Bioengineering*, 114(1), 172–183. <https://doi.org/10.1002/bit.26056>
- Datsenko, K. A., & Wanner, B. L. (2000). One-step inactivation of chromosomal genes in *Escherichia coli* K-12 using PCR products. *Proceedings of the National Academy of Sciences*, 97(12), 6640–6645. <https://doi.org/10.1073/pnas.120163297>
- Dong, H., Cui, Y., & Zhang, D. (2021). CRISPR/Cas technologies and their applications in *Escherichia coli*. *Frontiers in Bioengineering and Biotechnology*, 9, 762676. <https://doi.org/10.3389/fbioe.2021.762676>
- Dumon-Seignovert, L., Cariot, G., & Vuillard, L. (2004). The toxicity of recombinant proteins in *Escherichia coli*: A comparison of over-expression in BL21(DE3), C41(DE3), and C43(DE3). *Protein Expression and Purification*, 37(1), 203–206. <https://doi.org/10.1016/j.pep.2004.04.025>
- Englaender, J. A., Jones, J. A., Cress, B. F., Kuhlman, T. E., Linhardt, R. J., & Koffas, M. A. G. (2017). Effect of genomic integration location on heterologous protein expression and metabolic engineering in *E. coli*. *ACS Synthetic Biology*, 6(4), 710–720. <https://doi.org/10.1021/acssynbio.6b00350>
- Fessner, N. D. (2019). P450 monooxygenases enable rapid late-stage diversification of natural products via C-H bond activation. *ChemCatChem*, 11(9), 2226–2242. <https://doi.org/10.1002/cctc.201801829>
- Girhard, M., Klaus, T., Khatri, Y., Bernhardt, R., & Urlacher, V. B. (2010). Characterization of the versatile monooxygenase CYP109B1 from *Bacillus subtilis*. *Applied Microbiology and Biotechnology*, 87(2), 595–607. <https://doi.org/10.1007/s00253-010-2472-z>
- Goormans, A. R., Snoeck, N., Decadt, H., Vermeulen, K., Peters, G., Coussement, P., Van Herpe, D., Beauprez, J. J., De Maeseneire, S. L., & Soetaert, W. K. (2020). Comprehensive study on *Escherichia coli* genomic expression: Does position really matter? *Metabolic Engineering*, 62, 10–19. <https://doi.org/10.1016/j.ymben.2020.07.007>
- Gottesman, S. (1996). Proteases and their targets in *Escherichia coli*. *Annual Review of Genetics*, 30(1), 465–506. <https://doi.org/10.1146/annurev.genet.30.1.465>
- Hannemann, F., Bichet, A., Ewen, K. M., & Bernhardt, R. (2007). Cytochrome P450 systems—Biological variations of electron transport chains. *Biochimica et Biophysica Acta (BBA) - General Subjects*, 1770(3), 330–344. <https://doi.org/10.1016/j.bbagen.2006.07.017>
- Hayashi, K., Morooka, N., Yamamoto, Y., Fujita, K., Isono, K., Choi, S., Ohtsubo, E., Baba, T., Wanner, B. L., Mori, H., & Horiuchi, T. (2006). Highly accurate genome sequences of *Escherichia coli* K-12 strains MG1655 and W3110. *Molecular Systems Biology*, 2, 20060007. <https://doi.org/10.1038/msb4100049>
- Hoang, T. T., Ma, Y., Stern, R. J., McNeil, M. R., & Schweizer, H. P. (1999). Construction and use of low-copy number T7 expression vectors for purification of problem proteins: Purification of *Mycobacterium tuberculosis* RmlD and *Pseudomonas aeruginosa* LasI and RhlI proteins, and functional analysis of purified RhlI. *Gene*, 237(2), 361–371. [https://doi.org/10.1016/S0378-1119\(99\)00331-5](https://doi.org/10.1016/S0378-1119(99)00331-5)
- Jiang, Y., Chen, B., Duan, C., Sun, B., Yang, J., & Yang, S. (2015). Multigene editing in the *Escherichia coli* genome via the CRISPR-Cas9 system.

- Applied and Environmental Microbiology*, 81(7), 2506–2514. <https://doi.org/10.1128/AEM.04023-14>
- Kang, D. G., Kim Y. K., & Cha, H. J. (2002). Comparison of green fluorescent protein expression in two industrial *Escherichia coli* strains, BL21 and W3110, under co-expression of bacterial hemoglobin. *Applied Microbiology and Biotechnology*, 59(4-5), 523–528. <https://doi.org/10.1007/s00253-002-1043-3>
- Khatri, Y., Schifrin, A., & Bernhardt, R. (2017). Investigating the effect of available redox protein ratios for the conversion of a steroid by a myxobacterial CYP260A1. *FEBS Letters*, 591(8), 1126–1140. <https://doi.org/10.1002/1873-3468.12619>
- Labun, K., Montague, T. G., Krause, M., Torre Cleuren, Y. N., Tjeldnes, H., & Valen, E. (2019). CHOPCHOP v3: Expanding the CRISPR web toolbox beyond genome editing. *Nucleic Acids Research*, 47(W1), W171–W174. <https://doi.org/10.1093/nar/gkz365>
- Li, Q., Sun, B., Chen, J., Zhang, Y., Jiang, Y., & Yang, S. (2021). A modified pCas/pTargetF system for CRISPR-Cas9-assisted genome editing in *Escherichia coli*. *Acta Biochimica et Biophysica Sinica*, 53(5), 620–627. <https://doi.org/10.1093/abbs/gmab036>
- Li, S., Du, L., & Bernhardt, R. (2020). Redox partners: Function modulators of bacterial P450 enzymes. *Trends in Microbiology*, 28(6), 445–454. <https://doi.org/10.1016/j.tim.2020.02.012>
- Li, Y., Yan, F., Wu, H., Li, G., Han, Y., Ma, Q., Fan, X., Zhang, C., Xu, Q., Xie, X., & Chen, N. (2019). Multiple-step chromosomal integration of divided segments from a large DNA fragment via CRISPR/Cas9 in *Escherichia coli*. *Journal of Industrial Microbiology and Biotechnology*, 46(1), 81–90. <https://doi.org/10.1007/s10295-018-2114-5>
- Liu, X., Li, F., Sun, T., Guo, J., Zhang, X., Zheng, X., Du, L., Zhang, W., Ma, L., & Li, S. (2022). Three pairs of surrogate redox partners comparison for Class I cytochrome P450 enzyme activity reconstitution. *Communications Biology*, 5(1), 791. <https://doi.org/10.1038/s42003-022-03764-4>
- Mairhofer, J., Scharl, T., Marisch, K., Cserjan-Puschmann, M., & Striedner, G. (2013). Comparative transcription profiling and in-depth characterization of plasmid-based and plasmid-free *Escherichia coli* expression systems under production conditions. *Applied and Environmental Microbiology*, 79(12), 3802–3812. <https://doi.org/10.1128/AEM.00365-13>
- Merck KGaA. (2011). *pET System Manual (11th Edition)*. Merck KGaA.
- Miroux, B., & Walker, J. E. (1996). Over-production of proteins in *Escherichia coli*: Mutant hosts that allow synthesis of some membrane proteins and globular proteins at high levels. *Journal of Molecular Biology*, 260(3), 289–298. <https://doi.org/10.1006/jmbi.1996.0399>
- Okshevsky, M., Xu, Y., Masson, L., & Arbour, M. (2023). Efficiency of CRISPR-Cas9 genetic engineering in *Escherichia coli* BL21 is impaired by lack of Lon protease. *Journal of Microbiological Methods*, 204, 106648. <https://doi.org/10.1016/j.mimet.2022.106648>
- Omura, T., & Sato, R. (1964a). The carbon monoxide-binding pigment of liver microsomes. I. Evidence for its hemoprotein nature. *Journal of Biological Chemistry*, 239(7), 2370–2378. <https://www.ncbi.nlm.nih.gov/pubmed/14209971>
- Omura, T., & Sato, R. (1964b). The carbon monoxide-binding pigment of liver microsomes. II. Solubilization, purification, and properties. *Journal of Biological Chemistry*, 239(7), 2379–2385. <https://www.ncbi.nlm.nih.gov/pubmed/14209972>
- Ou, B., Garcia, C., Wang, Y., Zhang, W., & Zhu, G. (2018). Techniques for chromosomal integration and expression optimization in *Escherichia coli*. *Biotechnology and Bioengineering*, 115(10), 2467–2478. <https://doi.org/10.1002/bit.26790>
- Park, J. W., Lee, J. K., Kwon, T. J., Yi, D. H., Kim, Y. J., Moon, S. H., Suh, H. H., Kang, S. M., & Park, Y. I. (2003). Bioconversion of compactin into pravastatin by *Streptomyces* sp. *Biotechnology Letters*, 25(21), 1827–1831. <https://doi.org/10.1023/A:1026281914301>
- Petzoldt, K., Annen, K., Laurent, H., & Wiechert, R. (1982). Process for the preparation of 11 β -hydroxy steroids US Pat. 4,353,985, Schering Aktiengesellschaft.
- Pflug, S., Richter, S. M., & Urlacher, V. B. (2007). Development of a fed-batch process for the production of the cytochrome P450 monooxygenase CYP102A1 from *Bacillus megaterium* in *E. coli*. *Journal of Biotechnology*, 129(3), 481–488. <https://doi.org/10.1016/j.jbiotec.2007.01.013>
- Pontrelli, S., Chiu, T. Y., Lan, E. I., Chen, F. Y. H., Chang, P., & Liao, J. C. (2018). *Escherichia coli* as a host for metabolic engineering. *Metabolic Engineering*, 50, 16–46. <https://doi.org/10.1016/j.mbsen.2018.04.008>
- Qi, L. S., Larson, M. H., Gilbert, L. A., Doudna, J. A., Weissman, J. S., Arkin, A. P., & Lim, W. A. (2013). Repurposing CRISPR as an RNA-guided platform for sequence-specific control of gene expression. *Cell*, 152(5), 1173–1183. <https://doi.org/10.1016/j.cell.2013.02.022>
- Reisch, C. R., & Prather, K. L. J. (2015). The no-SCAR (Scarless Cas9 Assisted Recombineering) system for genome editing in *Escherichia coli*. *Scientific Reports*, 5, 15096. <https://doi.org/10.1038/srep15096>
- Richter, D., Bayer, K., Toesko, T., & Schuster, S. (2019). ZeBRa a universal, multi-fragment DNA-assembly-system with minimal hands-on time requirement. *Scientific Reports*, 9(1), 2980. <https://doi.org/10.1038/s41598-019-39768-0>
- Ro, D. K., Paradise, E. M., Ouellet, M., Fisher, K. J., Newman, K. L., Ndungu, J. M., Ho, K. A., Eachus, R. A., Ham, T. S., Kirby, J., Chang, M. C. Y., Withers, S. T., Shiba, Y., Sarpong, R., & Keasling, J. D. (2006). Production of the antimalarial drug precursor artemisinic acid in engineered yeast. *Nature*, 440(7086), 940–943. <https://doi.org/10.1038/nature04640>
- SaiSree, L., Reddy, M., & Gowrishankar, J. (2001). IS186 insertion at a hot spot in the *lon* promoter as a basis for *lon* protease deficiency of *Escherichia coli* B: Identification of a consensus target sequence for IS186 transposition. *Journal of Bacteriology*, 183(23), 6943–6946. <https://doi.org/10.1128/JB.183.23.6943-6946.2001>
- Seo, J.-H., Baek, S.-W., Lee, J., & Park, J.-B. (2017). Engineering *Escherichia coli* BL21 genome to improve the heptanoic acid tolerance by using CRISPR-Cas9 system. *Biotechnology and Bioengineering*, 22(3), 231–238. <https://doi.org/10.1007/s12257-017-0158-4>
- Studier, F. W. (2014). Stable expression clones and auto-induction for protein production in *E. coli*. In *Structural Genomics: General Applications* (pp. 17–32). Humana Press. https://doi.org/10.1007/978-1-62703-691-7_2
- Studier, F. W., & Moffatt, B. A. (1986). Use of bacteriophage T7 RNA polymerase to direct selective high-level expression of cloned genes. *Journal of Molecular Biology*, 189(1), 113–130. [https://doi.org/10.1016/0022-2836\(86\)90385-2](https://doi.org/10.1016/0022-2836(86)90385-2)
- Sudhamsu, J., Kabir, M., Airola, M. V., Patel, B. A., Yeh, S. R., Rousseau, D. L., & Crane, B. R. (2010). Co-expression of ferrochelatase allows for complete heme incorporation into recombinant proteins produced in *E. coli*. *Protein Expression and Purification*, 73(1), 78–82. <https://doi.org/10.1016/j.pep.2010.03.010>
- Ting, W.-W., Tan, S.-I., & Ng, I. S. (2020). Development of chromosome-based T7 RNA polymerase and orthogonal T7 promoter circuit in *Escherichia coli* W3110 as a cell factory. *Bioresources and Bioprocessing*, 7(1), 54. <https://doi.org/10.1186/s40643-020-00342-6>
- Urlacher, V. B., & Girhard, M. (2019). Cytochrome P450 monooxygenases in biotechnology and synthetic biology. *Trends in Biotechnology*, 37(8), 882–897. <https://doi.org/10.1016/j.tibtech.2019.01.001>
- von Böhler, C., Le-Huu, P., & Urlacher, V. B. (2013). Cluster screening: An effective approach for probing the substrate space of uncharacterized cytochrome P450s. *ChemBioChem*, 14(16), 2189–2198. <https://doi.org/10.1002/cbic.201300271>

- Wang, J., Niyompanich, S., Tai, Y. S., Wang, J., Bai, W., Mahida, P., Gao, T., & Zhang, K. (2016). Engineering of a highly efficient *Escherichia coli* strain for mevalonate fermentation through chromosomal integration. *Applied and Environmental Microbiology*, 82(24), 7176–7184. <https://doi.org/10.1128/AEM.02178-16>
- Yoon, S., Han, M.-J., Jeong, H., Lee, C., Xia, X.-X., Lee, D.-H., Shim, J., Lee, S., Oh, T., & Kim, J. F. (2012). Comparative multi-omics systems analysis of *Escherichia coli* strains B and K-12. *Genome Biology*, 13(5), R37. <https://doi.org/10.1186/gb-2012-13-5-r37>
- Zanos, P., Moaddel, R., Morris, P. J., Georgiou, P., Fischell, J., Elmer, G. I., Alkondon, M., Yuan, P., Pribut, H. J., Singh, N. S., Dossou, K. S. S., Fang, Y., Huang, X. P., Mayo, C. L., Wainer, I. W., Albuquerque, E. X., Thompson, S. M., Thomas, C. J., Zarate Jr., C. A., & Gould, T. D. (2016). NMDAR inhibition-independent antidepressant actions of ketamine metabolites. *Nature*, 533(7604), 481–486. <https://doi.org/10.1038/nature17998>
- Zanos, P., Moaddel, R., Morris, P. J., Riggs, L. M., Highland, J. N., Georgiou, P., Pereira, E. F. R., Albuquerque, E. X., Thomas, C. J., & Zarate, Jr. C. A., & Gould, T. D. (2018). Ketamine and ketamine

metabolite pharmacology: Insights into therapeutic mechanisms. *Pharmacological Reviews*, 70(3), 621–660. <https://doi.org/10.1124/pr.117.015198>

SUPPORTING INFORMATION

Additional supporting information can be found online in the Supporting Information section at the end of this article.

How to cite this article: Luelf, U. J., Böhmer, L. M., Li, S., & Urlacher, V. B. (2023). Effect of chromosomal integration on catalytic performance of a multi-component P450 system in *Escherichia coli*. *Biotechnology and Bioengineering*, 120, 1762–1772. <https://doi.org/10.1002/bit.28404>